Fuel 259 (2020) 116022

Contents lists available at ScienceDirect

Fuel

journal homepage: www.elsevier.com/locate/fuel

Full Length Article

Automated image analysis techniques to characterise pulverised coal particles and predict combustion char morphology

Joseph Perkins[a], Orla Williams[a], Tao Wu[b], Edward Lester[a,*]

[a] Faculty of Engineering, University of Nottingham, University Park, NG7 2RD Nottingham, United Kingdom
[b] Department of Chemical and Environmental Engineering, The University of Nottingham Ningbo China, Ningbo 315100, PR China

ARTICLE INFO

Keywords:
Coal characterisation
Macerals
Char morphology
Automated image analysis
Combustion
Vitrinite

ABSTRACT

A new automated image analysis system that analyses individual coal particles to predict daughter char morphology is presented. 12 different coals were milled to 75–106 μm, segmented from large mosaic images and the proportions of the different petrographic features were obtained from reflectance histograms via an automated Matlab system. Each sample was then analysed on a particle by particle basis, and daughter char morphologies were automatically predicted using a decision tree-based system built into the program. Predicted morphologies were then compared to 'real' char intermediates generated at 1300 °C in a drop-tube furnace (DTF). For the majority of the samples, automated coal particle characterisation and char morphology prediction differed from manually obtained results by a maximum of 9%. This automated system is a step towards eliminating the inherent variability and repeatability issues of manually operated systems in both coal and char analysis. By analysing large numbers of coal particles, the char morphology prediction could potentially be used as a more accurate and reliable method of predicting fuel performance for power generators.

1. Introduction

Despite a general decline in demand (mainly across Europe) over the last decade, coal is still used extensively to meet over a quarter of global power generation demands [1] and a key energy source for rapidly urbanizing and industrializing economies. As such, coal will remain a major baseline contributor to power generation for the foreseeable future during the transition of the energy mix towards more low carbon energy sources [2]. In optimising coal combustion for power generation and emission targets, generators increasingly need to understand the consequences of fuel choice to maximise the return on shipments, meet stringent NOx and SOx limits [3,4], and minimise shut down time for fouling and slagging maintenance, whilst maximising the potential for ash sales [5]. Thus, the ability to predict how the combustion performance of coals that are available on the market is valuable information to power generator, particularly coals with little documented burnout history.

The prediction of coal combustion performance has been attempted via several approaches over the years. Laboratory techniques include the use of characterisation techniques of physical properties such as volatile matter [6] and ash content [5], fuel ratio [6], particle size distribution [6,7] and intrinsic reactivity of char intermediates [8,6]. Visual petrographic methods of predicting coal combustion performance include rank [11], vitrinite reflectance [12], full maceral reflectance [9,10], maceral content [11], and maceral microlithotypes [12]. Currently, there is no technique for collating all these parameters together into a single predictive technique. This is most likely due to the heterogenous structure of coal, the complexity of maceral reactivity and performance dependence on coal origin and combustion process variables and conditions [9,10].

The ability to accurately predict the char morphology distribution for a given coal would be of particular use during the fuel selection process and when making coal burnout predictions, as the general rate of the combustion reaction is determined by the structure of these 'daughter' particles [10,13]. It is generally agreed that the rate of char oxidation is dependent on the heat transfer and the diffusion of reactant gases through 1) the char surface and 2) the char pore structures to permit the chemisorption of these gases and desorption of combustion products [12,14,15]. The performance of a particular coal in a furnace will therefore depend on how it reacts during pyrolysis and combustion.

Three fundamental chars characteristics have been taken as key differentiators: porosity, pore structure and wall thickness [6,16]. Chars have subsequently classified as either thin walled 'tenui-', thick walled 'crassi-' or solid/fused type structures [12,17], the assumption that thin chars will burn out more rapidly than thick chars has been applied to several char combustion modelling systems [14,15]. These char

* Corresponding author.
E-mail address: Edward.Lester@nottingham.ac.uk (E. Lester).

https://doi.org/10.1016/j.fuel.2019.116022
Received 31 May 2019; Received in revised form 9 August 2019; Accepted 13 August 2019
Available online 19 September 2019

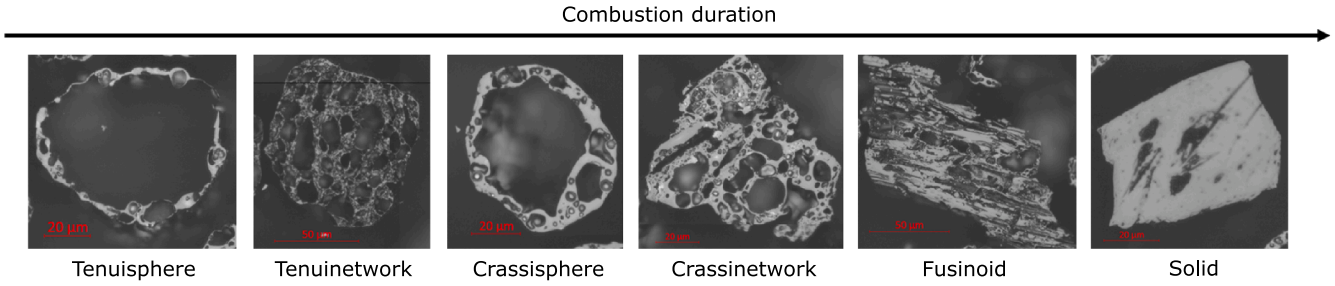

Fig. 1. ICCP morphologies moving from the thinnest walled to thickest walled chars.

morphologies are dependent on the original coal's characteristics, such as maceral type, rank, particle size, mineral matter and on process variables such as formation temperature, heating velocity, gaseous atmosphere and residence time [12,14,18,19]. Generally, the more reactive liptinite and vitrinite macerals will produce thinner combustion intermediates that burn more efficiently than those derived from inertinite [20–23]. Rank affects the reactivity of the maceral groups, with increasing reflectance corresponding to a decrease in reactivity [9]. Many of these original coal characteristics, such as rank, maceral content, %Unreactives and particle size/shape are measurable using rapid and automatable image analysis (IA) techniques [24–27], yet there is no automated image-based predictive method. This is possibly due to hardware and software limitations, the complexity of coal structure, requiring a trained petrographer, and the effects of origin on the pyrolysis behaviour of coal [7,9,28,29].

The potential of IA as a characterisation tool has advanced rapidly in recent years with the development of camera technology, computer processing power and IA software capabilities. Mineral Liberation Analysis (MLA Computer Controlled Scanning Electron Microscopy (CCSEM)) [30,31] is a well-established technique for imaging and characterising mineral content. Maceral detection using SEM is difficult owing to the similarity of maceral backscatter signals [32]. However, recently mineral detection combined with semi-automated maceral classification has been undertaken using traditional microscopy [33]. Furthermore, IA is already being used to characterise the coking potential of coal on a particle by particle basis [33,34]. With recent advances in IA, where process variables are assumed to be constant, automated coal characterisation and daughter char morphology prediction should be possible. An automated IA method would present several advantages over manual and semi-automated techniques. Point counting manual petrographic analysis has remained popular due to the reliability and precision that results from a well-standardised method [35–37] albeit labour and time intensive, with substantial allowable % error [38].

Semi-automated histogram analysis can reduce time requirements but it still relies on a skilled petrographer to ascertain maceral thresholds and verify the results [39]. A fully automated coal characterisation technique has the potential to be a more repeatable and faster analytical process [33].

This study describes the implementation of a new automated image analysis system using Matlab to accurately characterise individual coal particles and predict their daughter char morphology. The automated coal data was first compared to manual petrographic analysis to ensure parity and then the automated data was used to predict char types. The predicted morphology datasets were then compared to an actual set of chars generated using a drop-tube furnace at 1300 °C, 200 ms and 1% oxygen.

2. Methodology

2.1. Coal sample maceral and rank characterisation

To test the versatility of the predictive method, eleven different coals and one coke with a wide variation in composition and reflectance were chosen and included samples from Colombia, Czech Republic, Russia, Indonesia, South Africa, Wales, Vietnam and a Chinese coke. The coke was used to increase the reflectance range of the suite of samples to well beyond the normal values for combustion coals in order to test the scope of the prediction system. The coal samples were first milled using a Humbolt vibratory disc mill and then dry sieved into 75–106 µm range using an Alpine Jet Sieve. Blocks of each of the coal samples were prepared using a mixture of powdered 'Simplex Rapid' polyester resin and the coal fuel in a 1:1 ratio w/w and ground flat using Silicon carbide paper (800/1200/2400) and polished using a colloidal silica solution (Struers, OP-S, 0.04 µm) on a Struers Rotopol Automated Polishing System.

2.2. Manual maceral and automated rank analysis

Manual maceral analysis was conducted on a Leitz Ortholux II POL-BK microscope as per British Standard 6127:3 [35] to determine the Liptinite, Vitrinite and Inertinite content of each coal. Inertinite macerals were sub-divided into semi-fusinite and fusinite – representing the main inertinite sub-macerals. Automated rank analysis was conducted on a Zeiss Imager M1 microscope using an 8 bit imaging Zeiss AxioCam of the blocks.

2.3. Thermogravimetric analysis of the coals

Thermogravimetric Analysis (TGA) was used to analyse thermal composition of the samples and provide accurate carbon contents of each mix. Thermal profiles were produced using TA Instruments Q500 TGA (New Castle, DE, USA). TGA tests used 10–15 mg of the milled sample. The method used was based on a slow pyrolysis method [40]. The sample was heated in a furnace at 5 °C.min^{-1} in 100 ml.min^{-1} of Nitrogen from atmospheric temperature to 900 °C, after which the gas was switched to air at 100 ml.min^{-1}. The composition of the samples is given by moisture, dry volatile, fixed carbon, and ash content [41].

2.4. Char sample preparation

1 g of each 75–106 µm sample was pyrolysed in a vertical drop-tube furnace (DTF) (Severn Thermal Solutions, R765A) operating at 1300 °C, with a 200 ms residence time, and air flow set to 1% oxygen [7,9,14]. After collection, the char samples were prepared in blocks using a liquid resin (EPOFIX, Struers Ltd.) and vacuum infused for 30 mins before being left to cure for 24 h.

2.5. Mosaic image capture

For the development of the automated IA system, large mosaics of the coal and corresponding the daughter char samples were obtained using a Zeiss Image M1 microscope with a 50x oil immersion objective (and an internal 10x lens) providing a total of 500x magnification. The Zeiss automated stage was used to generate a 30 × 30 mosaic, representing a total area of 4.75 mm × 3.6 mm.

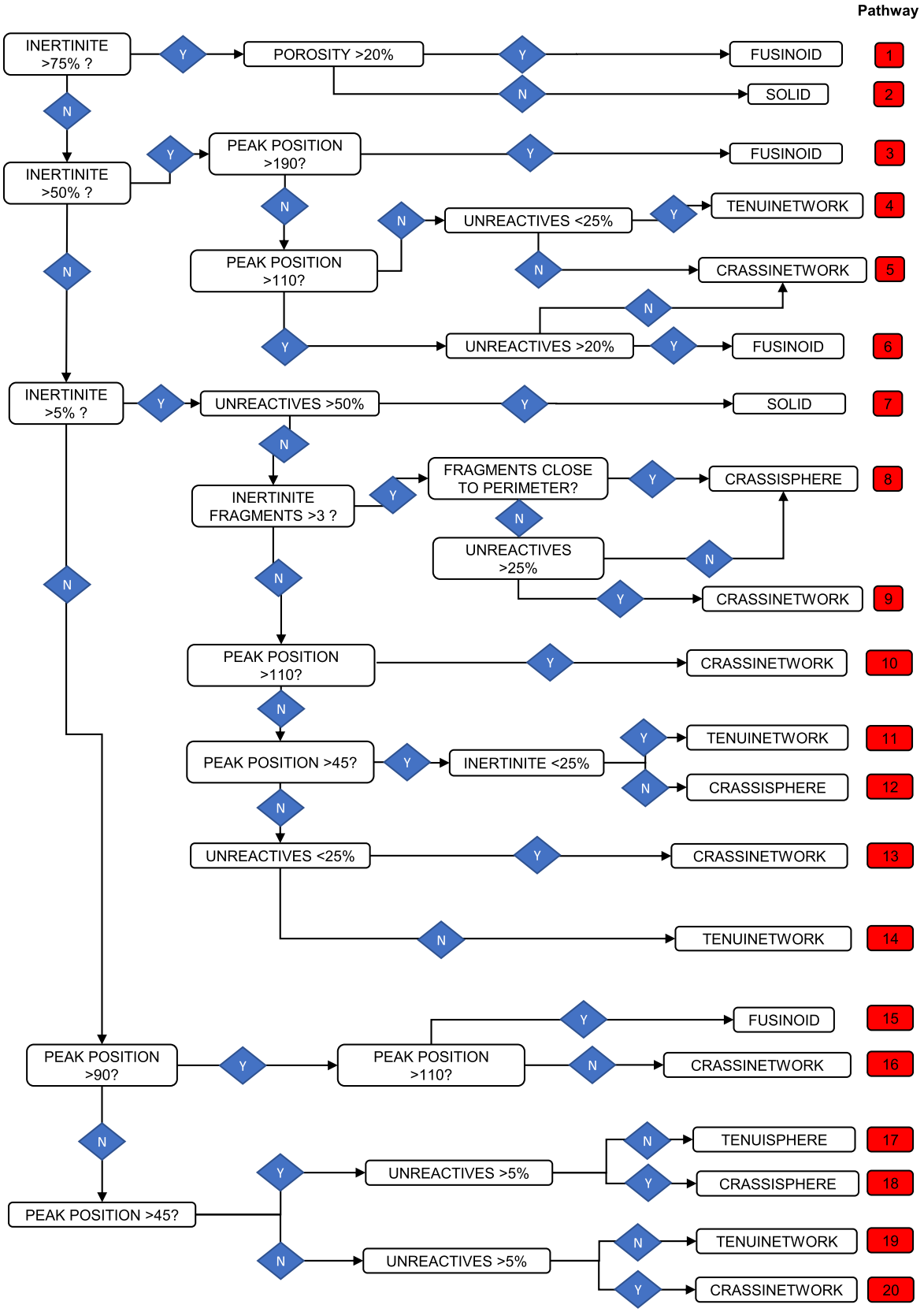

Fig. 2. Char morphology prediction decision tree.

3. Char morphology predictive system

Based on the assumption that thinner chars (that have proportionally more carbon material near the particle perimeter) burn faster than thicker chars [42], the morphologies can be ranked generally from fastest to slowest as shown in Fig. 1. For char morphology prediction, a decision based system (Fig. 2) was devised using the maceral distribution, rank, individual pixel greyscale values and the %Unreactives

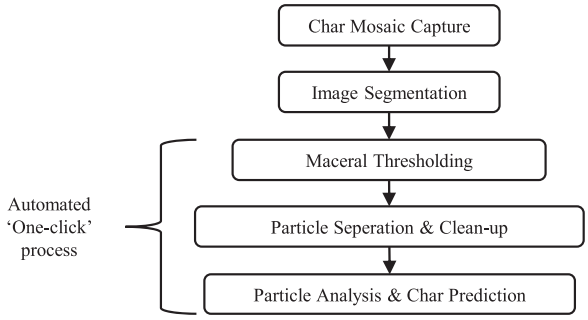

Fig. 3. Process flow for image analysis characterisation and prediction technique.

of each coal particle image to predict the different char morphologies as described in the International Committee for Coal and Organic Petrology (ICCP) Char Atlas [17], which was implemented in Matlab as a decision tree.

3.1. Maceral content

The predictive system classified each coal particle into high (> 75%), medium (> 50%), low (> 5%) and very low (0–5%) inertinite content categories due to the general trend of high inertinite content particles generally producing thicker and slower burning char morphologies, with the prevalence of faster burning morphologies increasing as inertinite content decreases [43].

3.2. Rank

Vitrinite is the maceral most influenced by changes in vitrinite reflectance (also referred to as rank) [44] and produces a variety of different char morphologies during pyrolysis [45]. Lower rank vitrinite generally produces more networked chars than higher ranked coals [46], with very high rank vitrinite showing little reactivity at all. Network-type chars were predicted for lower reflectance coal particles, and sphere-type morphologies predicted for higher reflectance vitrinite.

3.3. Percentage unreactives

The final morphology predictions were also dependant on the amount of unreactive material (%Unreactives) in the coal [10,16]. % Unreactives accounts for high reflectance macerals which have been shown to be lower in reactivity and produce slow burning char [13]. It has been previously shown that the %Unreactives parameter can be used to predict thickness of daughter chars for bituminous coal and the lower the %Unreactives the thinner the char type produced [32]. Whilst the %Unreactives parameter links to burnout, it is not sufficient (as a single number) to predict char morphology outright. However, char wall thickness can be related to this value [20], it provides a useful criterion for differentiating between thick and thin morphology predictions when combined with rank and quantities of inertinite.

4. Image analysis techniques

An outline of the automated IA process is shown in Fig. 3. After microscope mosaic capture, the image segmentation was a semi-automated process using Matlab with an operator ensuring that the thresholds had been correctly determined after segmentation. The coal maceral thresholding, particle separation, analysis and char morphology prediction was a continuous automated process and was implemented using Matlab 2018a + image processing toolbox add-on.

4.1. Semi-automated image segmentation

After initial image capture, the first step in the IA process was the accurate segmentation of the particles from the background resin. Attempts to remove the resin by traditional thresholding processes or traditional edge detection (ie. Canny edge detection [47]) can prove difficult due to the overlap of resin grayscale values with that of the coal particles, particularly those corresponding to liptinite and subsurface blemishes, either standalone or attributed to partly exposed polished particles.

The segmentation process itself was twofold. A variant of the Lazy Snapping Algorithm [48] was first used to separate foreground and background values into distinct areas using a K-means method [49], which removes background pixels as well as removing sub-surface and unfocused areas from around exposed particles (Fig. 4).

The Lazy Snapping method also segmented any background resin that was present within the particle boundaries. To remove this residual resin, a K-means clustering method which clusters pixels based on their intensity and neighbouring associations was used to determine the resin greyscale threshold (Fig. 5). 20 clusters proved effective enough to remove residual resin and leave liptinite mostly untouched. The binary mask generated was then overlaid on the original, unaltered mosaic, to generate a masked segmented image.

4.2. Automated particle separation & clean up

To separate touching and overlapping coal particles were the binary sample mask was subjected to a Watershed Transformation [50] (Fig. 6). The watershed transform finds "watershed ridge lines" in an image by treating it as a surface where light pixels represent high elevations and dark pixels represent low elevations. For a binary image such as the coal mosaic mask, a distance transform function [51] generated the topography in the image and any minima within the image would constitute the most likely area where two particles are touching. Whilst this method is generally successful with most touching particles, it does not work well where long edges are touching or where there was no obvious catchment basin. These were removed by a particle size filter and from the predictive process along with any small blemishes also liberated by the separation function.

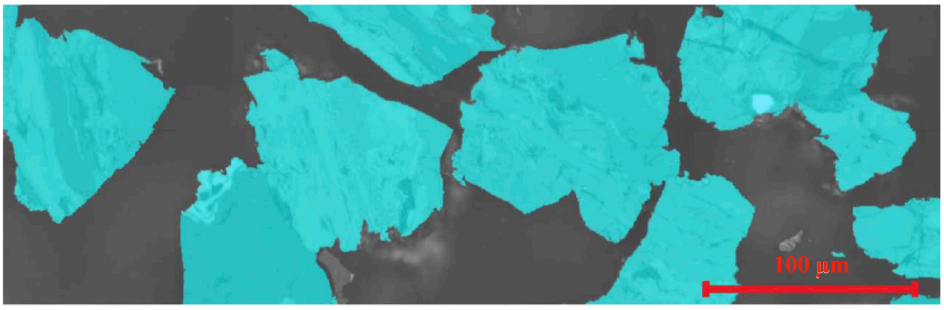

Fig. 4. Lazy Snapping segmentation of coal particles.

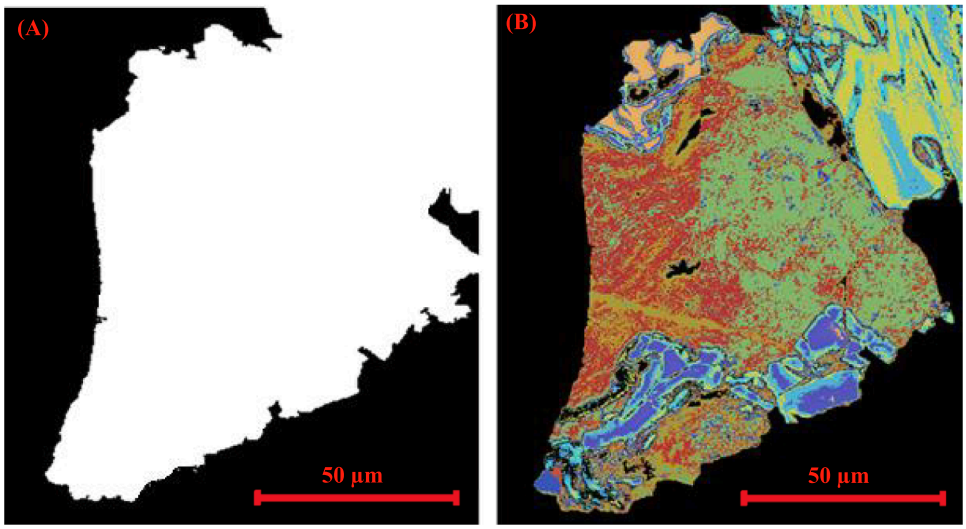

Fig. 5. Clustering segmentation of residual background resin. A) Lazy snapping segmentation result with residual resin and B) Clustering result showing with residual resin removed.

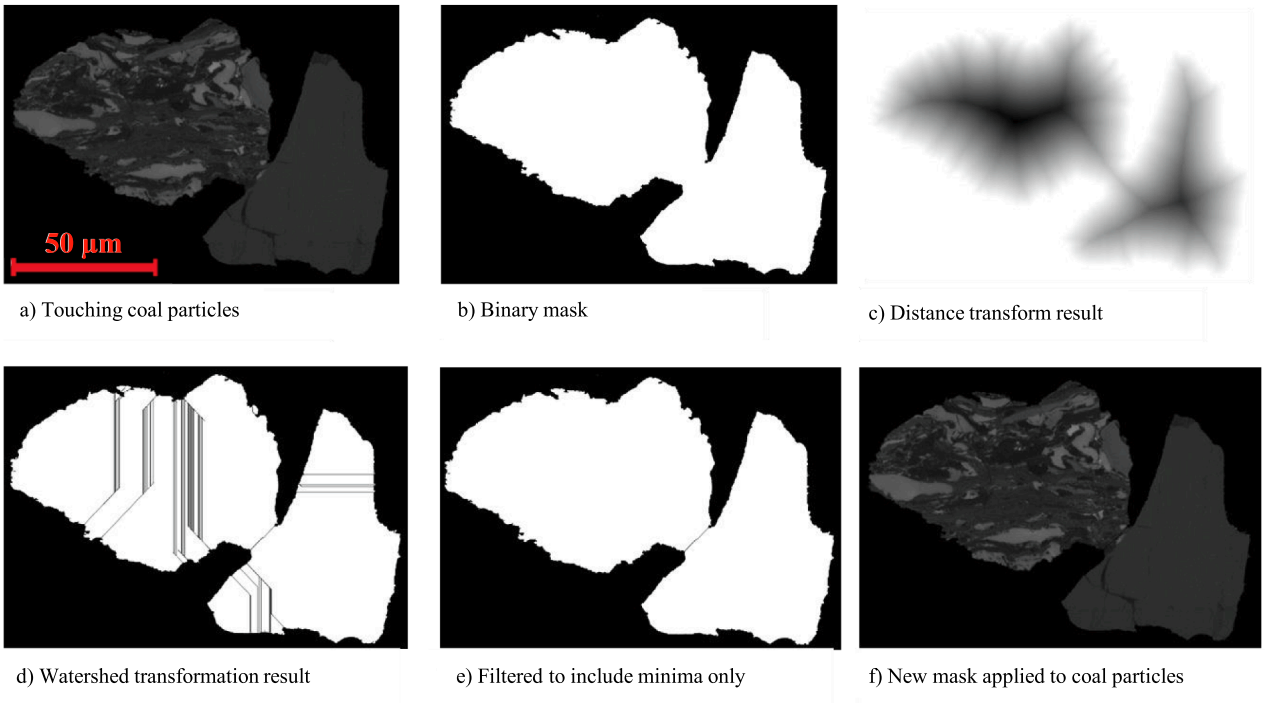

Fig. 6. Touching particle separation via distance transform and watershed transformations.

4.3. Automated maceral thresholding

The maceral thresholds were obtained using the greyscale histogram of the segmented mosaic. Firstly, the liptinite threshold was determined by the presence of any minima in the greyscale region below the vitrinite peak. The minima was calculated using a triangle threshold method [52] which computes the maximum distance between the histogram plot and a line from 0 to the vitrinite peak value.

It is thought that the threshold between vitrinite and inertinite lies within the semi-fusinite group, a maceral intermediate with properties between inertinite and vitrinite [53]. Depending on the rank of the sample, the peaks for vitrinite and semi-fusinite can be well separated or lie partially or directly over each other and the automated classification system determined the inertinite threshold depending on the shape of the reflectance histogram as follows;

1) **'No Overlap'** – The histogram plot is bimodal (i.e. there is a significant reflectance difference between vitrinite and semi-fusinite) then a value corresponding to 30% of the semi-fusinite peak height was found to match the manually obtained data closest.
2) **'Partial Overlap'** – There is some peak overlap but there remains a distinct transition point from vitrinite to inertinite, the threshold was set as half-way between the peaks due to increased overlap of higher reflectance vitrinite with semi-fusinite.
3) **'Complete overlap'** – If the vitrinite peak almost or completely conceals the semi-fusinite peak then a value corresponding to 28% of the vitrinite peak height was found to correlate with manual maceral data.

A graphical representation of the different histogram profiles and threshold locations is shown in Supplementary Figs. S1–4.

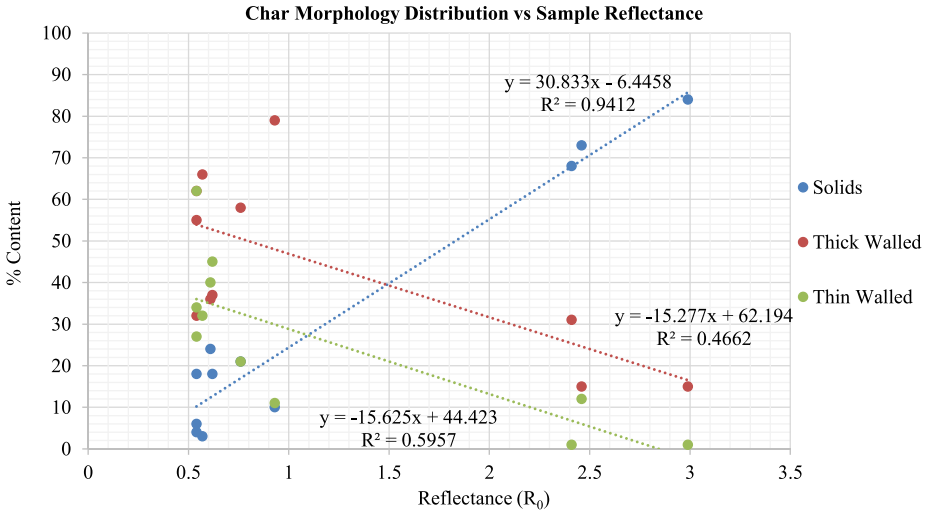

Fig. 7. Relationship between reflectance and general char morphology for 'real' chars generated in DTF.

4.4. Automated particle analysis and char morphology prediction

During the predictive process, each segmented and separated particle was automatically uploaded and analysed in a loop using Matlab to determine peak vitrinite position and maceral composition from the particle histogram, the position of the maceral components and the percentage of pixels that fall above the reactive threshold (set by % Unreactives) [10]. These values were then fed into the prediction decision tree model (Fig. 2), which was trained using Mathwork's Classification Learner using an initial dataset of manually compiled input values for the criteria outlined in 3.1–3.3 and their corresponding char morphology outputs.

5. Results & discussion

5.1. Proximate analysis

The proximate analysis data and vitrinite reflectance data for the 12 samples is presented in Supplemental Table 1. The vitrinite reflectance (for the coals) shows a wide range of values from La Loma at 0.51% through to the Vietnamese anthracite at 2.99%. The Chinese coke has a typical reflectance value around 7%. Clearly the proximate contents (particularly the fuel ratio) correlate with these vitrinite reflectance values but this has been described earlier [54].

5.2. Manual vs predicted maceral analysis

Supplementary Table 2 shows a good correlation between the automated and predicted maceral distributions was observed with 9 of the 11 coal samples differing by < 5%, and all 11 differing by < 10%. From ISO standards for petrographic analysis, these results would be considered to be comparable [38,55]. Image analysis can now provide a rapid and repeatable alternative to traditional maceral analysis to provide more reliable and comparable information. With the exception of the very high reflectance (%R_o = 2.46) Welsh sample 1 and the Chinese coke material, the automated thresholding method proved to be an effective tool to threshold a wide variety of coal samples into their major maceral constituents. Given that allowable operator-based manual point counting results between users for a maceral determined to be 50% of the sample, can fall between 43% and 57%, a variance of 5% from manually determined data using this method is well within the acceptable boundary of error [38]. In the case of the Welsh coal, the very high vitrinite reflectance resulted in a significant overlap of the vitrinite and semi-fusinite peaks, which is a limitation to a greyscale based automated thresholding. In this case, a trained operator would be required to distinguish between the semi-fusinite and vitrinite by way of morphological differences.

Whilst constituting the smallest percentage of the coal matrix, the classification of the liptinite maceral illustrated the largest relative discrepancy between manual and automated results. For the Indonesian and Klein Kopje samples, the predicted value was lower than the manual value, due to the variation in over segmentation during the K-mean clustering step, where too much liptinite is being removed along with residual background resin. There are many ways around this problem including colour imaging with fluorescence lighting [56], morphology manipulation [57] and air objectives [33]. However, as liptinite does not form a critical component in this predictive system and so it was of little consequence to the char morphology prediction processes. The characterisation system was unable to characterise the Chinese coke sample, not least because of the position of the reflectance peaks and absence of macerals. A separate characterisation system would be required to accurately characterise coke material with a different light setting and polarised optical filters.

5.3. Manual vs automated char prediction

The char morphology prediction results are summarized in Supplemental Tables 3 and 4. Table 3 shows a strong correlation between the manually analysed 'real' char and the predicted morphologies. However with certain specific char morphologies (most notably the tenuisphere and crassinetworks), there was variation of up to 16% between manual and predicted results. These observations indicate that there are still factors that were not measured by image analysis discussed in Section 1.

Table 4 shows a simple version of the data in Table 3 where general wall thickness is used to combine the 6 different morphologies i.e. 'thin', 'thick' and 'solid'. In all 12 carbon samples the predictions are within 8% of the manual data which is an excellent correlation between predicted and measured values.

Generally, as rank increases, char reactivity decreases due to the increasing prevalence of thicker and solid pyrolysis products (Fig. 7), a trend that supports previous research [10–13]. The relationship is strongest for the 'solids' grouping and higher reflectance samples, whereas there is more variation observed for the lower reflectance samples. This is entirely due to changes in maceral composition. Vitrinite reflectance can show trends between coals across a wide reflectance range but it is not sufficient as a parameter to predict char morphology at low rank ranges. Maceral composition can vary widely between two coals, even though the vitrinite reflectance is the same, and therefore both coals would generate quite different char types. e.g

the Russian and Indonesian samples produced a relatively high proportion of solid chars (~18%) despite their low rank. In terms of the three general morphology groupings, the predicted distributions of 'thin', 'thick' and 'solid' char morphologies are very close to those from those generated in the DTF with a maximal variance of 9% (Fig. 8a-c).

The largest discrepancies occurred in the lower reflectance coals, particularly those from Colombia. La Loma, El Cerrejon, Calenturitas all possess very similar proximate analysis, peak vitrinite values (42–45), vitrinite contents (88%, 90% & 90% respectively), however their chars generated in the DTF display very different distributions with La Loma producing a high proportion of tenuinetworks (40%) and crassispheres (26%), with El Cerrejon favouring tenui-(24%) and crassispheres (46%) and Calenturitas devolatilising to crassispheres (45%) and an even spread of networks. The prediction system accurately predicted the proportion of crassispheres for all these coals via route 8 (Fig. 2), however when it came to predicting char morphologies for those particles containing a high proportion of vitrinite (routes 15–20), there were significant discrepancies between predicted and manual results for tenuispheres, and networks. El Cerrejon for example, despite being very low rank, produced a higher proportion of 'Sphere' type chars (~70%) compared to the higher rank La Loma (~45%), contrary to previous work discussed earlier that indicated network-type structures should have been the preference. These variances can be attributed to natural variance due to the presence of inertodetrinite which can influence char morphology [58]. As the predictive system cannot currently account for these differences, a disparity was observed between manual and predicted results for some morphologies. For the higher rank coals; Ostrava, Zondag and Klein Kopje, the manual and predicted results were close, with a maximal variance range of just 7%. These coals do not tend to contain inertodetrinite and the % of inertinite is an accurate parameter in the predictive logic tree. Despite the note variations in the 6 specific char classes, the overall proportions of predicted 'thin', 'thick' and 'solid' char morphologies remain very close to these 'real' chars.

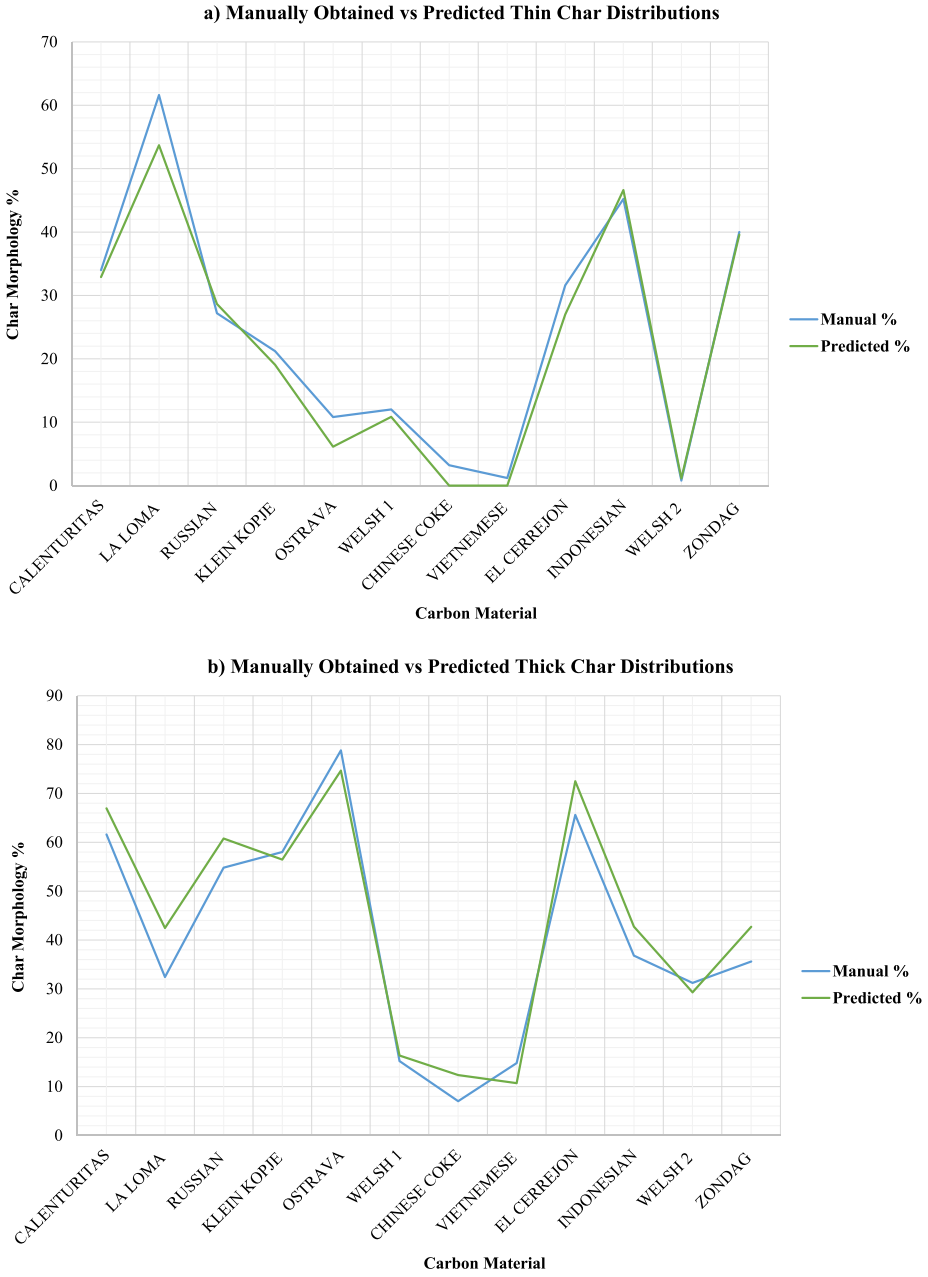

Fig. 8. a-c – Comparison between manual and predicted data for a) thin, b) thick and c) solid chars.

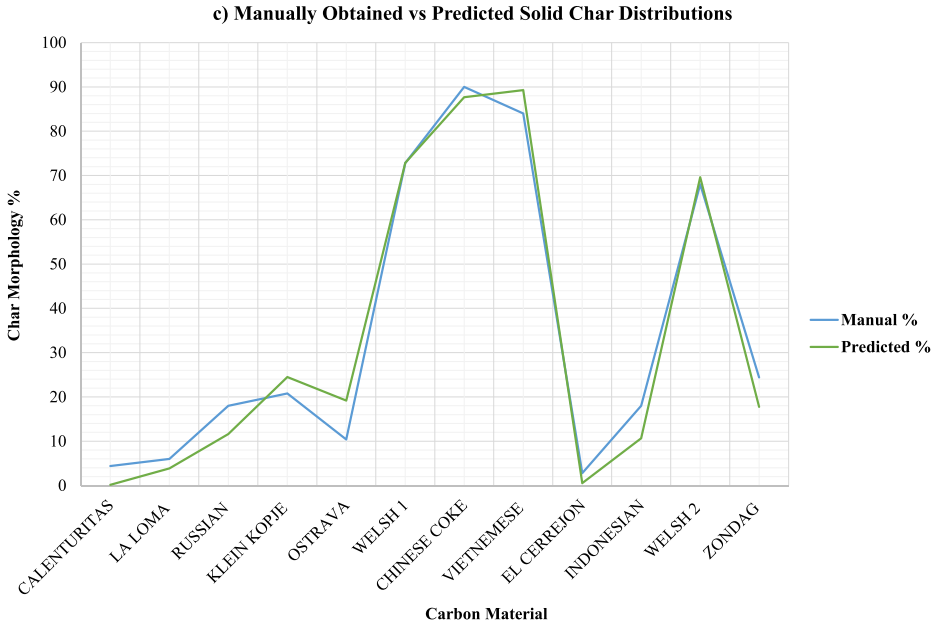

Fig. 8. (*continued*)

6. Conclusions and future work

A new image-based coal characterisation system to predict char morphology has been devised and developed. The system can separate coal particles and automatically segregate the particles into macerals groups and measure other features such as the dispersion of macerals within each particle. The predicted maceral composition vs actual composition appeared to be within standard prescribed by ISO standard.

The system then uses the information gathered from individual coal particles including reactivity (%Unreactives), inertinite content (with positional data) and vitrinite reflectance to predict char type.

In addition to rapid fuel characterisation, this IA system can predict the distribution of major char morphologies, matching closely with actual chars generated using a drop-tube furnace. This data could be used in the future by generators who are interested in predicting combustion characteristics of unknown coals.

Acknowledgements

This work was funded by the EPSRC Centre for Doctoral Training in Carbon Capture and Storage and Cleaner Fossil Energy [grant number EP/L016362/1].

Appendix A. Supplementary data

Supplementary data to this article can be found online at https://doi.org/10.1016/j.fuel.2019.116022.

References

[1] Agency IE. Coal Report 2017: Analysis and Forecasts to 2022. 2017.
[2] Committee, M.C.E.S.A., The Future of Coal 2003.
[3] Directive 2008/50/EC of the European Parliament and of the Council of 21 May 2008 on ambient air quality and cleaner air for Europe. 2008, Official Journal of the European Union. p. Chapter 15 Volume 029 P. 169–212.
[4] Regulation (EU) No 525/2013 of the European Parliament and of the Council of 21 May 2013 on a mechanism for monitoring and reporting greenhouse gas emissions and for reporting other information at national and Union level relevant to climate change and repealing Decision No 280/2004/EC. 2013, Official Journal of the European Union. p. Chapter 15 Volume 031 P. 251–278.
[5] Jayaranjan MLD, van Hullebusch E, Annachhatre A. Reuse options for coal fired power plant bottom ash and fly ash. Vol. 13. 2014.
[6] Wells WF, Smoot LD. Relation between reactivity and structure for coals and chars. Fuel 1991;70(3):454–8.
[7] Cloke M, Lester E, Belghazi A. Characterisation of the properties of size fractions from ten world coals and their chars produced in a drop-tube furnace. Vol. 81. 2002. 699–708.
[8] Avila C, et al. Morphology and reactivity characteristics of char biomass particles. Bioresour Technol 2011;102(8):5237–43.
[9] Lester E, Cloke M. Characterisation of coals and their respective chars formed at 1300°C in a drop tube furnace. Vol. 78. 1991. 645–1658.
[10] Cloke M, Lester E, Gibb W. Characterization of coal with respect to carbon burnout in p.f.-fired boilers. Fuel 1997;76(13):1257–67.
[11] Su S, et al. A proposed maceral index to predict combustion behavior of coal. Fuel 2001;80(5):699–706.
[12] Bailey JG, et al. A char morphology system with applications to coal combustion. Fuel 1990;69(2):225–39.
[13] Cloke M, Lester E, Thompson AW. Combustion characteristics of coals using a drop-tube furnace. Fuel 2002;81(6):727–35.
[14] Cloke M, et al. Char characterisation and its application in a coal burnout model☆. Fuel 2003;82(15):1989–2000.
[15] Benfell KE, et al. Modeling char combustion: the influence of parent coal petrography and pyrolysis pressure on the structure and intrinsic reactivity of its char. Proc Combust Inst 2000;28(2):2233–41.
[16] Borrego AG, Alvarez D, Menéndez R. Effects of inertinite content in coal on char structure and combustion. Energy Fuels 1997;11(3):702–8.
[17] Alvarez DL, E, Atlas of Char Occurrences. 2001: Combustion Working Group, Commission III. ICCP.
[18] Jones RB, Morley C, McCourt CB. Maceral effects on the morphology and combustion of coal char. 1985.
[19] Lee B. et al., Effect of coal properties on combustion characteristics in a pulverized coal fired furnace. Vol. 33. 2009. 737–747.
[20] Wu T, Lester E, Cloke M. A burnout prediction model based around char morphology. Energy Fuels 2006;20(3):1175–83.
[21] P., J., A new classification system for biomass and waste materials for their use in combustion. 2016, University of Nottingham.
[22] Nandi BN, Brown TD, Lee GK. Inert coal macerals in combustion. Fuel 1977;56(2):125–30.
[23] Smoot LD. Fundamentals of coal combustion: for clean and efficient use. Amsterdam; New York: Elsevier; 1993.
[24] Riepe W, Steller M. Characterization of coal and coal blends by automatic image analysis: use of the Leitz texture analysis system. Fuel 1984;63(3):313–7.
[25] Chao ECT, Minkin JA, Thompson CL. Application of automated image analysis to coal petrography. Int J Coal Geol 1982;2(2):113–50.
[26] David P, Fermont W. Application of colour image analysis in coal petrology. Vol. 20. 1993. 747–758.
[27] Wu T, Lester E, Cloke M. Advanced automated char image analysis techniques. Energy Fuels 2006;20(3):1211–9.
[28] Sarofim AF, Bar-Ziv E. The influence of coal type on the evolution of polycyclic aromatic hydrocarbons during coal devolatilization AU – Mitra, Amitava. Aerosol Sci Technol 1987;6(3):261–71.
[29] Michele GD, Riccardi J, Lopez-Doriga E. Influence of coal type and operating conditions on the formation of incomplete combustion products. Pilot plant experiments AU – BONFANTI, L. Combust Sci Technol 1994;101(1–6):505–25.
[30] Waanders F, Mulaba-Bafubiandi A, Lodya L. The South African industry use of

Mössbauer spectroscopy to solve operational problems. Vol. 226. 2013. 721–735.
[31] Wells J. et al., The nature of mineral matter in a coal and the effects on erosive and abrasive behaviour. Vol. 86. 2005. 535–550.
[32] Cardott B, Curtis ME. Identification and nanoporosity of macerals in coal by scanning electron microscopy. Vol. 190. 2017.
[33] O'Brien G. et al., Semi-automated petrographic assessment of coal by coal grain analysis. Vol. 20. 2007. 428–434.
[34] Comino P, Warren K, O'Brien G. Applying the Coal Grain Analysis (CGA) method on liberation studies in coal. 2010.
[35] British Standard (BS) 6127, 1982. Petrographic analysis of bituminous coal and anthracite, Part 3: Method of determining maceral group composition of bituminous coal and anthracite, Database Section, BSI Milton Keynes, Milton Keynes, U.K.
[36] British Standard (BS) 6177, 1981. Petrographic analysis of bituminous coal and anthracite Part 2: Method of preparing coal samples for petrographic analysis. Database Section, BSI Milton Keynes, Milton Keynes, U.K.
[37] Materials, A.S.o.T., in Microscopical determination of volume percent of physical components in a polished specimen of coal. 1980: Philadelphia, Pa.
[38] Bustin RM. Quantifying macerals: some statistical and practical considerations. Int J Coal Geol 1991;17(3):213–38.
[39] Lester E, et al. An automated image analysis system for major maceral group analysis in coals. Fuel 1994;73(11):1729–34.
[40] Lester EGM, Thompson A. A method for source apportionment in biomass/coal blends using thermogravimetric analysis. Anal Appl Pyrolysis 2007;80:111–7.
[41] Institution, B.S., Coal – proximate analysis, in BS ISO 17246. 2010.
[42] Lester E, Cloke M, Allen M. Char characterization using image analysis techniques. Energy Fuels 1996;10(3):696–703.
[43] Rojas-González AF, Barraza J. Volatile matter release and thin and thick char formation as a function of vitrinite content, coal rank, time and temperature devolatilization. Ingeniería y competitividad 2013;15:171–9.
[44] Oka N, et al. The influence of rank and maceral composition on ignition and char burnout of pulverized coal. Fuel Process Technol 1987;15:213–24.
[45] Rojas A, Barraza J. Caracterización morfológica del carbonizado de carbones pulverizados: estado del arte. Revista Facultad de Ingeniería Universidad de Antioquia 2007:84–97.
[46] Vargas D, et al. Beneficiated coals' char morphology. Ingeniería e Investigación 2013;33:13–7.
[47] Canny J. A computational approach to edge detection. IEEE Trans Pattern Anal Machine Intelligence 1986;PAMI-8(6):679–98.
[48] Li Y, et al. Lazy snapping. ACM Trans Graph 2004;23(3):303–8.
[49] MacQueen J. Some methods for classification and analysis of multivariate observations. Proceedings of the fifth Berkeley symposium on mathematical statistics and probability, Volume 1: Statistics. Berkeley, Calif.: University of California Press; 1967.
[50] Meyer F. Topographic distance and watershed lines. Signal Process 1994;38(1):113–25.
[51] Maurer Calvin R, Qi R, Raghavan V. A linear time algorithm for computing exact euclidean distance transforms of binary images in arbitrary dimensions. IEEE Trans Pattern Anal Mach Intell 2003;25(2):265–70.
[52] Zack GW, Rogers WE, Latt SA. Automatic measurement of sister chromatid exchange frequency. Vol. 25. 1977. 741–53.
[53] The new inertinite classification (ICCP System 1994). Fuel, 2001. 80(4): p. 459–471.
[54] Stach E, T.b.M.-T.M., Teichmüller M, et al. a.E.r.b.D.G. Murchison, Stach's textbook of coal petrology. 1982.
[55] ISO 7404-3 – Methods for the petrographic analysis of bituminous coal and anthracite – Part 3: Method of determining maceral group composition. 1994.
[56] Cloke M, et al. Automated maceral analysis using fluorescence microscopy and image analysis. Vol. 74. 1995. 659–669.
[57] Lester E. et al. An automated image analysis system for major maceral group analysis in coals. Vol. 73. 1994. 1729–1734.
[58] Neomagus H. et al. Properties of high ash char particles derived from inertinite-rich coal: 1. Chemical, structural and petrographic characteristics. Vol. 87. 2008.